RSC Advances

ROYAL SOCIETY OF CHEMISTRY

www.rsc.org/advances

Cite this: DOI: 10.1039/c0xx00000x

www.rsc.org/xxxxxx

ARTICLE TYPE

Microstructural Transition of Aqueous CTAB Micelles in Presence of Long Chain Alcohol

Jasila Karayil,[a] Sanjeev Kumar,[b] P. A. Hassan,[c] Yeshayahu Talmon,[d] and Lisa Sreejith*[a]

Received (in XXX, XXX) Xth XXXXXXXXX 20XX, Accepted Xth XXXXXXXXX 20XX

DOI: 10.1039/b000000x

The effect of long chain alcohols (C_9OH-$C_{12}OH$) on the micellar properties of CTAB in the presence of inorganic salt, KBr have been systematically studied by viscometry, rheology, DLS and direct imaging technique cryo-TEM. The molar ratio of CTAB/KBr was fixed at 1:1 and the alcohol concentration range from 0.005-0.03M. With increase in concentration of the alcohol, the Mitchell-Ninham surfactant parameter, R_p increases favouring micellar growth as noted in the results of the viscosity studies with a peaked behaviour followed by a drop (regions I-III). In region I the sample is less viscous and have propensity to form short cylindrical micelles. The rheological response of samples at the plateau region (region II) showed strong viscoelasticity indicating the presence of wormlike micelles, which was confirmed by cryo-TEM and DLS analysis. A drop in viscosity (region III) was observed at still higher concentration of alcohol. The increase in apparent hydrodynamic diameter of the micelles with concentration of alcohol confirm the alcohol induced micelle growth. An unusual temperature response was another feature noticed for C_9OH samples in region III and the cryo-TEM investigation revealed the presence of vesicles which are nearly absent in C_{10}-$C_{12}OH$.The results thus suggest the strong dependence of the surfactant morphologies on the solubilisation site of added alcohol which could be further affected by temperature.

Introduction

The self-assembly of surfactant molecule utilizes non-covalent interactions such as hydrophobic vander Waals, hydration and electrostatic[1-3]. The micro structure of the self-assembly can be correlated to Mitchell-Ninham parameters, R_p[4] which depend up on the effective ratio of volume (v), length (l) of alkyl tail part to the head group area (a_o) for a typical surfactant ($R_p = v / a_o l$). Fang and Venable used R_p to explain a series of structural transitions[5]. Size and shape of the micelle were found to affect the counter-ion condensation in micellar head group region [8]. Inorganic and organic counter-ions were reported to induce micellar growth due to screening of the electrostatic repulsion between the head groups (decrease in a_o and hence increase R_p)[6,7]. The partitioning of organic additives into head group region can also modify inter-head group repulsion together with increase in v, leading to increase in R_p [9]. This increase in R_p facilitates the formation of various morphologies consistent with the geometrical packing model of Israelachvili et al [10].

Extensive work has been done on the effect of different additives on the micellar morphologies [11-14]. Alcohols are one of the widely used additives added to surfactant to form microemulsions[15]. Depending upon the hydrophobicity of alcohol, the added alcohol can locate/partition either on the micellar surface, palisade layer and/or core (Fig. 1). The locus of the alcohol solubilisation in micelle is the main governing factor to determine its action on surfactant systems [16]. The effect of short and medium chain alcohols on the micellar growth of ionic micelles have been investigated using a variety of techniques[17-20]. It was noticed that short chain alcohols (n< 3) tend to remain in the aqueous phase, alter the hydrogen-bonded structure of water, thereby disrupts the micelles and decreases hydrodynamic diameter of micelles[21].The aforementioned behaviour was reported recently by Taliha et al[22]. They found that addition of (C_1OH to C_3OH) to micellar solution leads to an increase in CMC and are less effective in inducing micellar growth in cationic surfactants. Medium chain alcohols (n>4) were found to intercalate between micelles (palisade layer) causing a decrease in CMC and thereby promote micellar growth[23-26]. Kuperkar and his co-workers[27]examined the effect of linear alcohols (C_2OH to C_6OH) on cationic surfactants and emphasise that on increasing the hydrocarbon chain length of alcohol (n) there is a marked decrease in CMC, resulting in pronounced micellar growth. Similar behaviour was reported for ionic micellar system with alcohol chain length up to C_8[14].Thus depending upon their carbon chain length (n), alcohol can act either as co-solvent or cosurfactant.

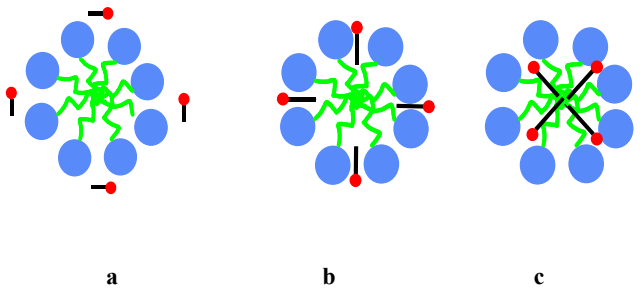

Figure 1: Schematics of location of the solubilisation of alcohols a) near micellar surface b) in the palisade region and c) in the micellar core. is alcohol of different chain length.

It is a well established fact that inorganic salt can enhance the effect of additives on the self assembling nature of surfactant. David et al[28] studied the synergistic effect of salt and alcohol on cationic surfactants and reported an enhancement of viscosity in the system. Added salt may affect the partitioning of alcohol between the micelle and aqueous phase[29]. It is thus of great interest to see how an additive at different micellar solubilisation sites can influence association morphology and its subsequent physical properties. It would then be easier to mimic more complex biological systems since they are having involvement of hydrophobic interactions like simpler surfactant morphologies (micelles or vesicles) [30-32].

There are only a few reports on the study of micellar transitions of CTAB in presence of long chain alcohol. Recently, we have initiated a study on micelle to vesicle transition (MVT) in CTAB/n-octanol/KBr system [33]. Further, a neutron scattering study showed that disk-like aggregates are present in a potassium dodecanoate-dodecanol-water system. It is expected that higher chain length alcohol can only be solubilised either in micellar palisade layer or in the core and can potentially increase the R_p at relatively lower concentration, as they are nearly insoluble in micellar background aqueous solution.Therefore, higher chain length alcohol can be the appropriate candidate to tune the R_p.

Above facts prompted us to carry out a systematic study on CTAB/KBr in presence of higher homologues of alcohols. This paper is the first ever report of the combined effect of long chain alcohols (C_9OH-$C_{12}OH$) and KBr on the structural transition of CTAB using viscosity, rheology, DLS and cryo-TEM techniques. We also monitored the viscosity behaviour of the above systems as a function of temperature ranging from 25-60°C. Few systems show pronounced viscosification on heating. Such thermo-responsive structural transitions are reported only for a few systems in the past [33-35]. Heating induced viscosity increase can be of importance in various biological and mechanical applications (micro fluidic devices and hydraulic fracturing) [36-38]. Therefore, material of the present study might make it attractive for some of these applications.

Experimental Sections

Materials

CTAB (Merck Germany, 99% assay), was purchased and used as received. All the additives used KBr (Himedia, 99% assay), n-nonanol (Merck, 99% assay), n-decanol (Merck, 99% assay), n-undecanol (Merck, 99% assay) and n-dodecanol (Merck, 99% assay) were of high purity chemicals and were used without further purification. The water used to prepare the solutions was Millipore Water of conductivity 18.2 MΩ.cm.

Sample Preparation

The stock solution was prepared by dissolving a weighed amount of CTAB and KBr in millipore water. The alcohols of varying concentration were added to this solution using glass microsyringe (Hamilton) and were heated to 50°C under continuous stirring for half an hour until the solution becomes homogeneous. The samples were then kept at room temperature for at least one day to attain equilibrium.

Rheology

Steady and dynamic rheological experiments were performed on a controlled stress rheometer (Anton Paar Physica MCR-301) with a parallel plate sensor (50-mm diameter). The gap was 1mm. Experiments were performed at 30 ± 0.01 °C. The viscosity of the sample was obtained from steady-shear measurements with the shear rate ranging from 0.3 to 500 s^{-1}. Frequency sweep measurements were performed at a given stress in the frequency region varying from 0.1 to 100 rad s^{-1}.The samples were equilibrated at least 15 minutes at measuring temperature prior to the measurement.

Viscosity Measurements

The absolute viscosity of samples under conditions of defined shear rate and shear stress were determined by a programmable Brookfield DV – II + cone and plate viscometer (Brookfield Engineering Laboratories, Inc - USA) thermostated at the temperature range 25-60 ± 1°C. Prior to the measurement samples were mounted at least 30 minutes to attain thermal equilibrium.

DLS measurements

Measurements were performed with a Malvern 4800 Autosizer employing a 7132 digital correlator at a scattering angle of 130°C. A vertically polarized light of wavelength 514.5 nm from an argon laser was used as the incident beam. All solutions were filtered with a 0.2 m membrane filter before the measurements to avoid interference from dust. The measured intensity correlation functions were analyzed by the method of cumulants33 where unimodal distribution of relaxation time is considered. The size distribution is obtained using the CONTIN algorithm, wherever needed.

Cryo TEM

Vitrified cryo-TEM specimens were prepared in a controlled environment vitrification system (CEVS), at 25°C and 100% relative humidity to avoid loss of volatiles, followed by quenching into liquid ethane at its freezing point. The specimens, kept below -178°C, were examined by an FEI T12 G2 transmission electron microscope, operated at 120 KV, using a Gatan 626 cryo-holder system. Images were recorded digitally on a Gatan US1000 high-resolution cooled-CCD camera using the

Digital Micrograph 3.4 software package in the low dose imaging mode.

Results and Discussion

Effect of concentration and chain length of alcohol on CTAB/KBr micellar system

Mukerjee[39]has pointed out, if an additive is surface active to a hydrocarbon-water interface, it will solubilise in the head group region (Fig. 1b) and may promote structural transitions. Greater partitioning of the additive to the interior (Fig. 1c) was shown to retard micellar growth by virtue of releasing the requirement of the monomer tails to reach the centre of the micelles and thus will swell[40,41]. Spherical micelles (R_P<1/3) were found to be less viscous whereas the wormlike micelles (1/3<R_P<1/2) showed pronounced viscosity. Hence, viscosity results provide an indication of structural transitions and can be used to study the morphological evolution in the surfactant solution [42].

0.1M CTAB/0.1KBr micellar solution is less viscous (≈10 cP), and has propensity to form spherical (or short rod shaped) micelles. However the addition of long chain alcohol to 0.1M CTAB/0.1KBr micellar solution dramatically increases its viscosity (≈17,500 cP). The zero shear viscosity (η_0) of aqueous 0.1 M CTAB / 0.1 M KBr with varying concentration of C_9OH-$C_{12}OH$ at different temperatures (25-60°C) is shown in Fig. 2 (a-d) and it is observed that η_0 is a strong function of concentration (C_0) and chain length (n) of alcohol (peaked behaviour). Three regions (region I-III) were identified and it was explained on the basis of formation of ordered structures / phase behaviour. At lower C_0 (<0.01M), viscosity increases distinctly which corresponds to the micellar elongation (region I). With increase in C_0, these micelles can grow anisotropically into cylindrical ones and at critical C_0, entangles to form a network of wormlike micelles with rapid increase in viscosity, η_0^{max} (region II). This C_0, at which the viscosity increases sharply, can be considered to be the concentration needed for sphere to rod transition (s→r).

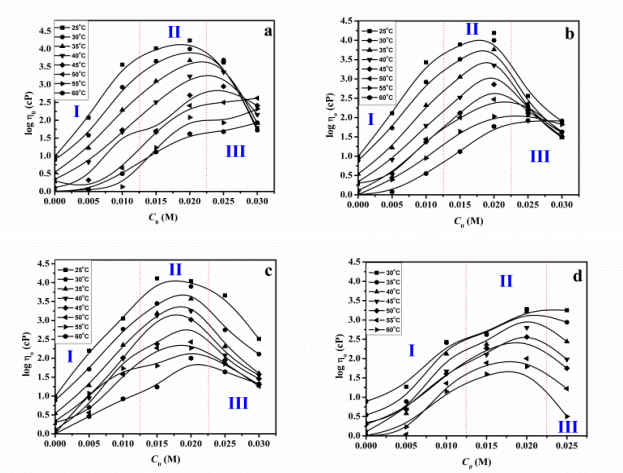

Figure 2: Effect of alcohol concentration (C_0) on the zero shear viscosity, log (cP) of 0.1MCTAB/0.1M KBr for (a) Nonanol (b) Decanol (c) Undecanol and (d) Dodecanol at temperatures ranging from 25-60°C.

Desai *et al*[43] has studied the (s→r) of CTAB in the presence of n-octanol and proposed that octanol forms alcohol-surfactant mixed micelles, reduces the repulsion between the charged head groups and thus modify the effective R_p, and is responsible for the micelle growth. When alcohol molecules are solubilised in micellar palisade layer (Fig. 1b), it will contribute towards the overall volume of a micelle, therefore, volume per surfactant monomer will effectively increase and is responsible for the increase in R_p. Similar analogy can be extended to other long chain alcohols used here and was believed to cause micellar growth due to decrease in electrostatic repulsion by KBr addition and increase of hydrophobic interaction by intercalation of alcohol molecules between monomers of the micelle (as R_p will also increase as mentioned above). On further addition of alcohol, the samples become less viscous and show a bluish hue (region III). The bluish colour is a manifestation of the Tyndall effect due to the presence of scatterers in solution, and it is generally seen for solutions containing vesicles.[44]

To better understand the rich variation in viscosity, we have performed rheological measurements with selected samples at 30°C. The steady shear viscosities obtained for the samples (≥0.01 M C_0) showed non-Newtonian behaviour (Fig. 3) i.e., the viscosity decreases drastically with an increase in shear rate (shear thinning behaviour). Upon increasing the concentration of alcohol the viscosity increases promptly: an indication of the formation of rigid rods of medium length, which slowly converts in to flexible wormlike micelles [45, 46]. Here the samples are clear and viscoelastic. However, at higher C_0 (0.03 M) shear thinning becomes less prominent (deviation from non-newtonian behaviour). The non-viscous and bluish nature of the sample solution reflects the presence of unilamellar vesicles.Vesicular dispersion is expected to be dilute, and therefore a nearly Newtonian behaviour without much variation in viscosity is observed [47,48]. A similar vesicular phase with n-decanol in sodium N-lauroylsarcosinate hydrate is already reported [49].

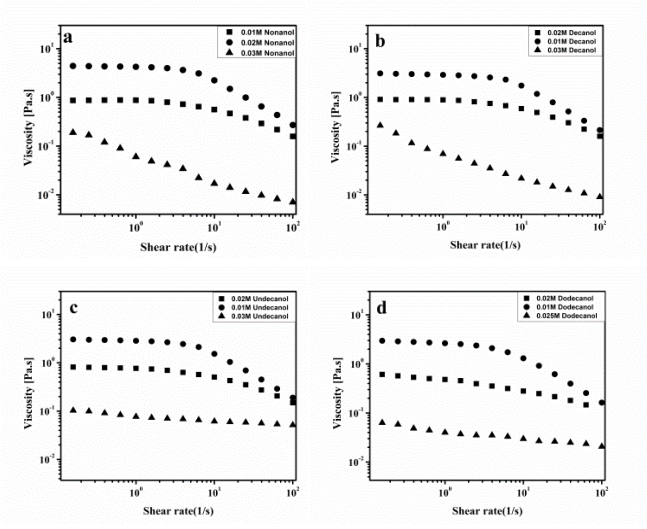

Figure 3: The Steady shear rheological response of 0.1M CTAB/0.1M KBr as a function of C_0 (a) Nonanol (b) Decanol (c) Undecanol and (d) Dodecanol ■ is 0.01M, ● is 0.02 M, ▲ is 0.03M alcohol respectively.

The viscoelastic properties of the samples were analyzed by oscillatory-shear experiments. The variation of elastic modulus (G') and viscous modulus (G") as a function of frequency (ω) at 30°C is given in Fig. 4.

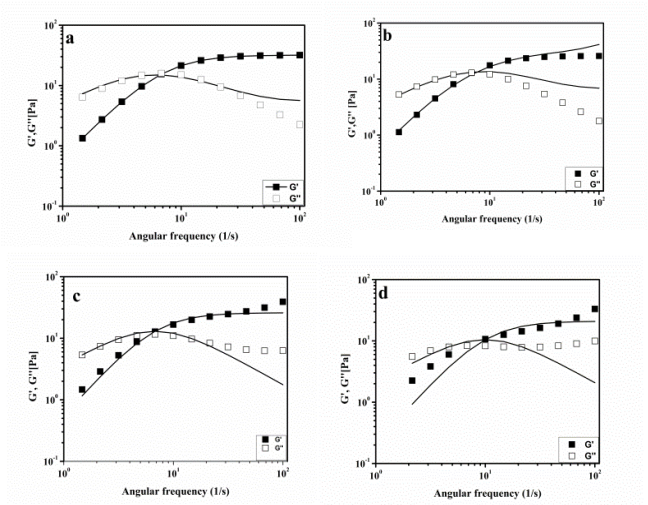

Figure 4: Dynamic rheological response of G' (closed) and G'' (open) for 0.1M CTAB/0.1MKBr at C_0 0.02M (a) Nonanol (b) Decanol (c Undecanol and (d) Dodecanol at 30 °C

The dynamic rheological response of the samples shows that, at high frequencies, it behaves elastically (G' > G"), while at low frequencies, it switches to a viscous behaviour (G" > G'), a typical viscoelastic behaviour shown by worm-like micellar solutions [9].The rheological behaviour of this system was characterized by the generalized Maxwell model. For a Maxwell fluid, the variation of the G' and G" can be given as [50, 51].

$$G'(\omega) = \frac{\omega^2\tau^2}{1+(\omega\tau)^2}G_0$$

$$G''(\omega) = \frac{\omega\tau}{1+(\omega\tau)^2}G_0$$

where, ω is the frequency, G_0 is the plateau modulus and τ the relaxation time. At lower frequency Maxwell behaviour with single relaxation time was observed for the samples and the data fits reasonably well in the Maxwell model.This behaviour in the low-frequency regime for viscoelastic fluids is usually demonstrated in a Cole-Cole plot of G' vs G" (Fig. 5). A semi-circular relationship over the majority of frequencies was noted for a Maxwell fluid [51, 52].The deviation of G" from the Maxwell model in the higher frequency region is another characteristic feature of the worm-like micelles. This observation corresponds to the fact that the worm-like micelles are in dynamic equilibrium and there is a rapid breaking and recombination process (shown by living polymers) [53].This is related to breathing or Rouse like motion [54].

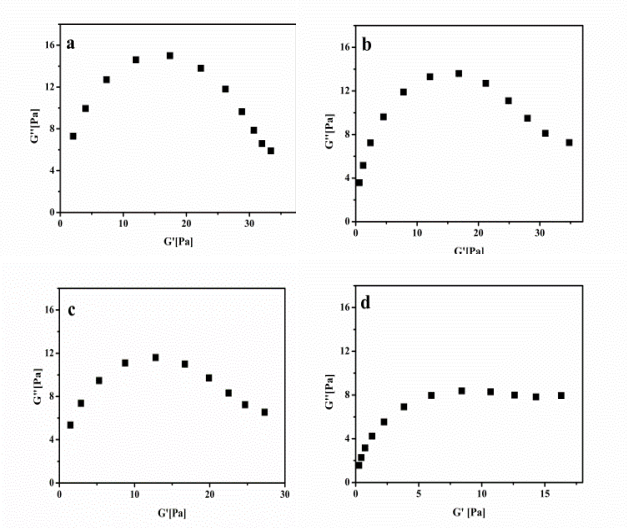

Figure 5: Cole-Cole plot for wormlike micelle solutions0.1MCTAB/0.1M KBr at C_0 0.02M (a) Nonanol (b) Decanol (c) Undecanol and (d) Dodecanol at 30°C

Shear plateau in wormlike micelles have been widely observed in the literature. Above a characteristic shear rate, the flow curve shows a plateau with a finite slope[55, 56].The nature of this behaviour as well as the mechanism at its origin is still the subject of intense debate. Cates et al [57]have proposed that the plateau is a signature of mechanical instability in the form of shear bands. Figure 6 shows the flow curve for 0.1M CTAB/0.1M KBr containing 0.02M C_9OH-$C_{12}OH$ at 30°C. The flow curve exhibits a discontinuity of slope at the critical value, followed by a stress plateau which persists over decades in strain rates. This further confirms the presence of wormlike micelles in the systems.

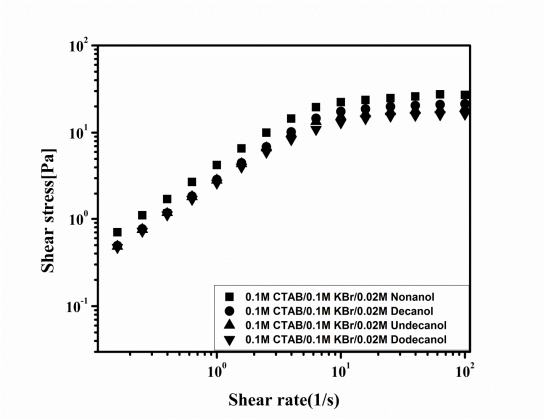

Figure 6: Shear stress as a function of the shear rate for 0.1M CTAB/0.1M KBr/0.02M C_9OH-$C_{12}OH$ at 30°C.

The hydrophobic interaction between the embedded alcohol and hydrocarbon part of micelles causes a reduction in the free energy of the micelles and can promote its growth. As a result the viscosity of system increases with increase in chain length. An increase in viscosity, on increasing the chain length of alcohol (n) from 9 to 12 was expected. However, steady-shear rheological data for the samples (Fig. 6) show that, there is viscosity drop on going from nonanol to dodecanol.The zero shear viscosity of CTAB/KBr/Nonanol system is 5 times higher than CTAB/KBr/dodecanol system (Fig.7a).Also the average relaxation time of CTAB/KBr/nonanol is greater than CTAB/KBr/dodecanol system (Fig. 7b). This could be due to the deeper penetration of dodecanol in CTAB micellar core (Fig. 8). Thus effectiveness of dodecanol to induce micellar growth diminishes since core solubilisation fail to cause much growth.

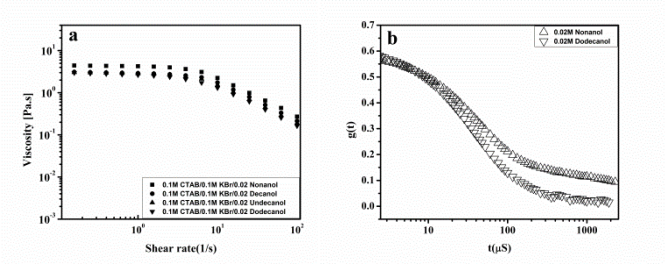

Figure 7 (a) The Shear viscosity of 0.1M CTAB/0.1MKBr/0.02M C_9OH-$C_{12}OH$ at 30°C (b) Variation of the electric field correlation function with time for 0.02M C_9OH and $C_{12}OH$.

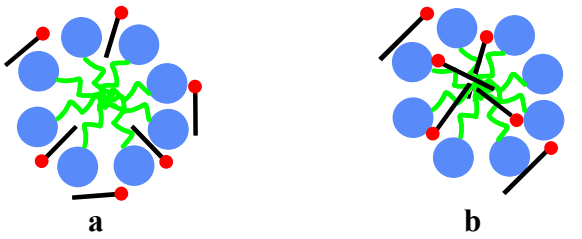

Figure 8: Schematic diagram for the proposed solubilisation site of Nonanol and Dodecanol in CTABr micelles.

DLS was employed to track the hydrodynamic diameter of the microstructures. DLS data for 0.1 M CTAB + 0.1 M KBr system show low hydrodynamic diameter in the absence of alcohol and is consistent with low viscosity as given in Fig. 2. With increase in concentration of alcohols the average hydrodynamic diameter of the micelle shift to larger diameter region (Fig. 9).

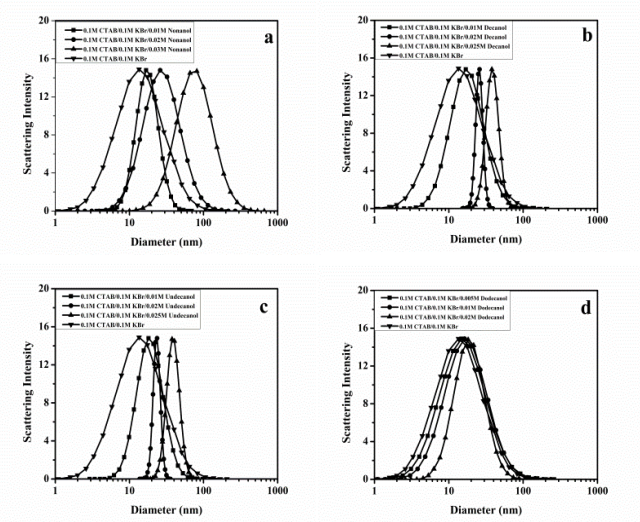

Figure 9: Intensity weighted distribution of apparent hydrodynamic diameter of 0.1MCTAB/0.1M KBr micellar solutions as a function of C_0 : (a) Nonanol (b) Decanol (c) Undecanol and (d) Dodecanol

Figure 10 shows the variation of the electric field correlation function in the presence of increasing concentration of alcohol. It is observed that the correlation function shifts to longer time with increasing concentration of alcohol. This indicates an increase in the average relaxation time with increase in concentration of alcohol, suggesting an increase in the average dimension of the micelles (micellar elongation).

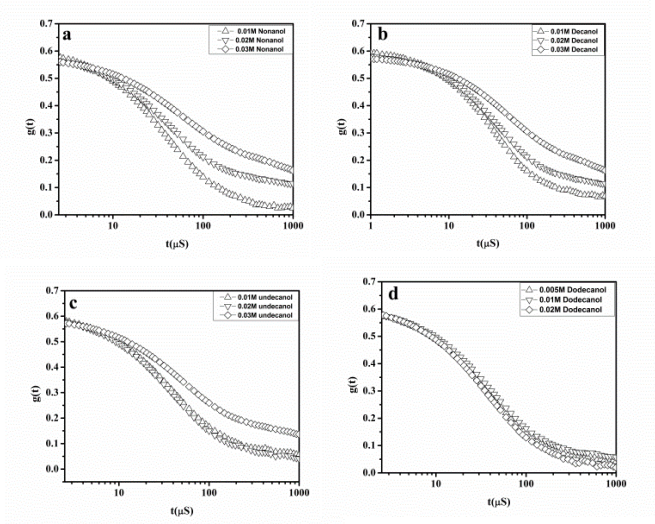

Figure 10: Variation of the electric field correlation function with time for 0.1 M CTAB/0.1 M KBr solution as a function of C_0 a) Nonanol, b) Decanol, c) Undecanol and d) Dodecanol.

Direct imaging cryo-TEM correlates the presented data with the microstructure of the micelles shown in different regions of Fig.1. Cryo-TEM examination of the samples in region II shows the presence of entangled network of worms with branching (Fig.

11). These wormlike micelles impart high viscosity to the system, and the solution becomes viscoelastic as observed in region II of Fig. 2 and by rheological studies (Fig. 4).

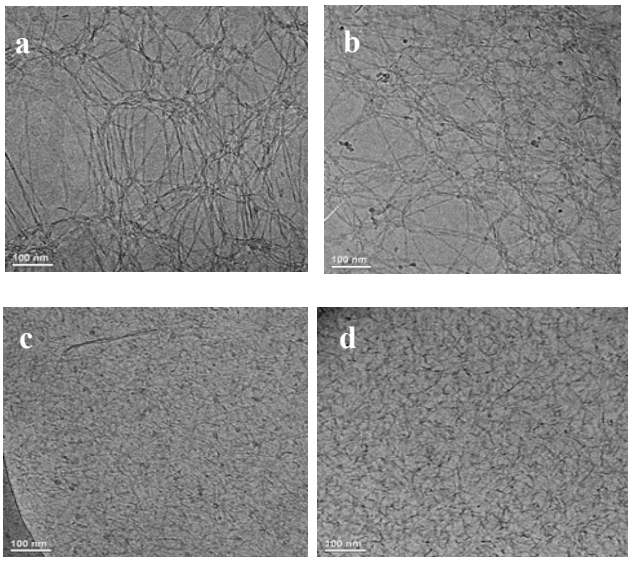

Figure 11: Cryo-TEM micrographs of wormlike micelles formed in 0.1MCTAB/0.1MKBr at C_0 0.02M (a) Nonanol, (b) Decanol, (c) Undecanol, and (d) Dodecanol. Scale bar 100 nm.

The Cryo-TEM images (Fig. 12) for samples from region III (C_0 = 0.03 M) depict the coexistence of wormlike micelles (arrow-1), unilamellar vesicles (arrow-2) and oligovesicles (arrow 3). To our surprise, wormlike micelle to vesicle transition was found only with additive, nonanol (Fig. 12a, 12b). This exclusive ability of nonanol to transform rod shaped micelles to vesicles is a complicated question to answer. A plausible explanation may be the distribution of nonanol between head group region and micellar core. Such distribution may impart flexibility to the aggregate to transform from rod shape micelle to the vesicle. It is expected that on initial addition of nonanol it may partition more in the micellar head group region which is responsible for the formation of rod or worm like micelle. However, at higher concentration one can expect nonanol partitioning towards interior or core of the micelle. These two partitioning sites (head group and interior regions) may be responsible for above transition. The values of the vesicular size obtained in the micrographs were in agreement with those obtained by other authors who investigated similar mixed micelle systems [58,59]. The other alcohol (C_{10}OH and C_{11}OH) incorporated samples at higher concentration causes breakdown of wormlike micelles to short cylinders, as clear from the respective cryo-TEM images (Fig. 12c, 12d). This behaviour can be explained in the light of increased hydrophobicity of higher chain length alcohols which force them to go into the micelle core. In this situation, structure / flexibility of the head group region would be affected. It has been reported that head group partitioning would always be responsible for micellar growth while interior solubilisation causes lower order aggregates. This indeed was observed in case of C_{10}OH and C_{11}OH (Fig. 12c and 12d).

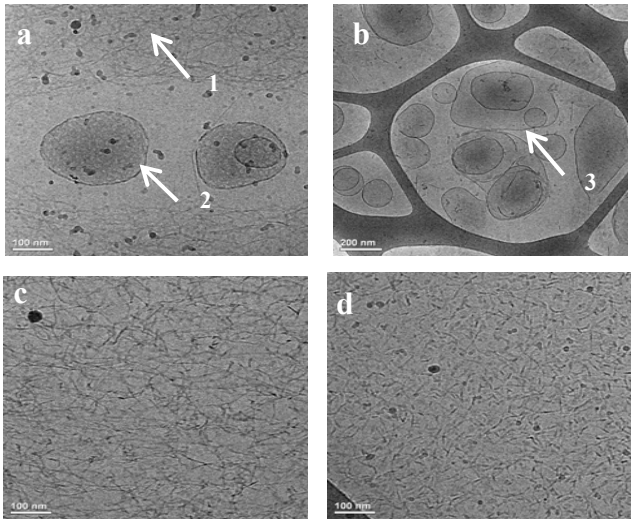

Figure 12: Cryo-TEM micrographs of samples located above the peak viscosity region C_0 0.03 M Nonanol at (a) scale bar 100 b) 200. The coexistence of threadlike micelles (arrow-1), unilamellar vesicles (arrow-2) and oligo vesicles (arrow 3) can be seen here. Elongated and short rod like micelles are the dominant microstructures for (c) 0.03M Decanol and (d) 0.03M undecanol.

Effect of Temperature

The behaviour of worm-like micelles greatly depends on temperature. The Arrehenius plot of log η_0 *vs* 1/T (where T is the absolute temperature) falls on a straight line (Fig.13), the slope of which yields the flow activation energy (E_a).Values of E_a ranging from 70 to 300 kJ/mol have been reported for various micellar solutions [60].The η_0 decreases with the rise of temperature showing that it decays exponentially with temperature.This exponential decay of viscosity with temperature is in accordance with Arrehenius type of equation for wormlike micelles [61].

$$\eta_0 = Ae^{-Ea/RT}$$

where, R is the universal gas constant and A is a Arrehenius constant.

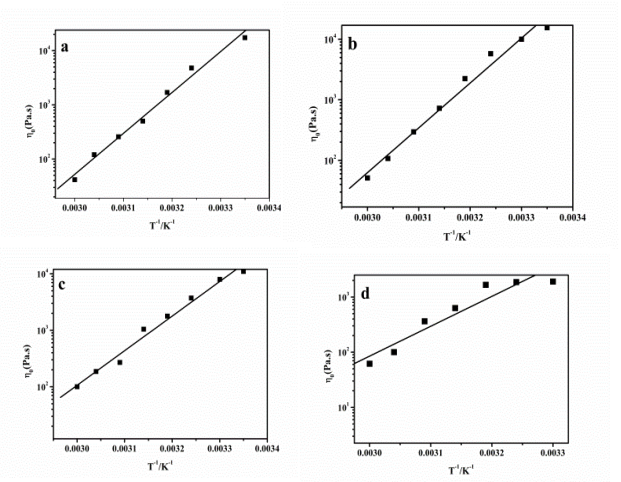

Figure 13: Effect of temperature on the zero-shear viscosity, η_0, versus 1/T on semilog scale for 0.1MCTAB/0.1MKBr systems at C_0 0.02M (a) Nonanol (b) Decanol (c) Undecanol (d) and Dodecanol. Solid lines are the fits to the data point.

The values of flow activation energies were determined from the slopes of the straight lines and calculated to 105, 102, 96 and 80kJ/mol for C_9OH to $C_{12}OH$, respectively. These values are comparable to the reported value (70-300 kJ/mol) for wormlike micelles obtained in other systems. It can be noted that CTAB/ KBr/Dodecanol system show large deviation from straight line, which shows that it is least viscoelastic among the other three systems. However, E_a values are also supports the formation of longer micelles as observed by other experimental data (viscometry, DLS and cryo-TEM).

An unusual thermo viscosification was observed for CTAB/KBr/0.03M Nonanol system. This micellar solution consists of vesicles, as demonstrated by cryo Tem. However, upon increasing the temperature, there is substantial increase in viscosity (~7 fold increase) and the sample turns into optically clear, viscous fluid.This is attributed to a micellar shape transition upon heating. Probably vesicle to rod like transition takes place with temperature. At higher temperature some of the nonanol molecules may leach out from the micellar interior to surface region, thereby decreasing the R_p and modify the morphology to rod like with a concomitant increase in viscosity (Fig. 2a, region III).

Conclusion

Cetyl trimethyl ammonium bromide in presence of additives (KBr and long chain alcohol) can show various microstructural transitions. We demonstrated that a small rod - wormlike - vesicle transformation of aggregate takes place with continuous increase of concentration of alcohol.These transitions take place within a narrow concentration range of alcohol (0.01–0.03 M). DLS data were complementary to viscosity and rheological data and support the micellar growth. Cryo-TEM data show the spontaneous formation of unilamellar, multilamellar, and oligovesicles in the 0.03 M nonanol system. However, such a rich morphological changes were absent with higher chain length alcohols.On combining the present results of nonanol with previous study,[33] it can be concluded that alcohol with chain length (n = 8 or 9) produces vesicles. Further, effectiveness of an additive to modify R_p value decides the overall morphology at a particular concentration.

Acknowledgements

We would like to acknowledge Dr. Ellina Kesselman, Dr. Judith Schmidt (Technion-Israel Institute of Technology) for their help in the Cryo-TEM analysis and Ms.Linet Rose J. for her help immense help in carrying out the rheological experiments.The research grant from UGC as a fellowship (19-12/2010(i) EU-IV) is also acknowledged.

Notes and references

[a]*Department of Chemistry, NIT Calicut, Kerala,India, E-mail: jessekarayil@gmail.com*
[b]*Department of Applied Chemistry, Faculty of Technology and Engineering,The Maharaja Sayajirao University of Baroda, Vadodara, India*
[c]*Chemistry Division, BARC, Mumbai, India.India .*
[d]*Department of Chemical Engineering, Technion-Israel Institute of Technology, Haifa, Israel.*
[*a]*Department of Chemistry, NIT Calicut, Kerala, India. Fax:* +91-495-22867280; Tel: +91-495-2286553; E-mail: lisa@nitc.ac.in.

1 D.Chandler, Nature, 2005, **437**, 640.
2 C. B. Minkenberg, L. Florusse, R. Eelkema, G. J. M. Koper, J. V. VanEsch, *J. Am. Chem. Soc.*, 2009, **11**, 11274.
3 S. Kumar, A. Bhadoria, H. Patel, V. K. Aswal, *J. Phys. Chem. B*, 2012, **116**, 3699.
4 D. J. Mitchell and B. W. Ninham, *J. Chem. Soc. Faraday Trans. 2*, 1981, **77**, 601.
5 J. Fang and R. L. Venable, *J. Colloid Interface Sci.*, 1987, **117**, 448
6 H. Rehage and H. Hoffman, *Mol. Phys.*, 1991, **74**, 933.
7 R. T. Buwalda, M. C. A. Stuart and J. F. B. Engberts, *Langmuir*, 2000, **16**, 6780
8 V. K. Aswal and P. S. Goyal, *Phys. Rev.*, 2000, **61**, 2947.
9 Z. Lin, J. J. Cai, L. E. Scriven and H.T. Davis, *J. Phys. Chem.*, 1994, **98**, 5984
10 J. N. Israelachvili, D. J. Mitchell and B. W. Ninham, *J. Chem. Soc. Faraday Trans.*, 1977, **72**, 1525.
11 S. Kumar, D. Sharma, G. Ghosh and Kabir-ud-Din, *Langmuir*, 2005, **21**, 9446.
12 N. Vlachy, M. Drechsler, J-M Verbavatz, D. Touraud and W. Kunz, *J. Colloid Interface Sci.*, 2008, **319**, 542.
13 R. Abdel-Rahem, *Adv. Colloid Interface Sci.*, 2008, **141**, 24.
14 Kabir-ud-Din, Z. A. Khan and S. Kumar, *Colloid Polym. Sci.*, 2008, **286**, 335.
15 P. Baglion and L. Keran, *J Phy Chem*, 1987, **91**, 1516.
16 M. Aamodt, M. Landgren, and B. Jonsson, *J. Phys. Chem.*, 1992, **96**, 945.
17 P. Sudheesh, S. M. Nair and L. Sreejith, *Asian J. Appl. Sci.*, 2008, **1**, 246.
18 Kabir-ud-Din, Z. A. Khan and S. Kumar, *Colloid Polym. Sci.*, 2008, **286**, 335.
19 P. M. Lindemuth and G. L. Bertrand, *J. Phys. Chem.*, **97**, 1993, 7769.
20 R. Zana, *Adv. Colloid and Interface Sci.*, 1995, **57**, l.
21 L. A. Moreira and A. Firoozabadi, *Langmuir*, 2009, **25**, 12101.
22 T. Sidim , G.Acar, *J Surfact Deterg* ,2013, **16**:60.
23 R. Zana, C. Picot and R. Duplessix, *J. Colloid and Interface Sci.*, 1983, **93**, 43.
24 B. Michels and G. Waton, *J. Phys. Chem.* B, 2003, **107**, 1133.

25 E. Hirsch, S. Candau, R. Zana, J. Colloid Interface Sci., 1984,**97**,318.
26 R. Zana, S. Yiv, C. Strazielle and P. Lianos, *J. Colloid and Interface Sci.*, 1981, **80**, 280.
27 K. C. Kuperkara,, J. P. Matab, P. Bahadur, Colloids and Surfaces A: Physicochem. Eng. Aspects 380 ,2011, 60.
28 S. L. David, S. Kumar and Kabir-ud-Din, *J. Chem. Eng. Data*., 1997, **42**, 198.
29 S. Kumar, Z. A. Khan and Kabir-ud-Din, *J. Surfactants and Deterg.*, 2002, **5**, 55.
30 C. Tanford, The Hydrophobic Effect: Formation Of Micelle And Biological Membranes, Wiley, New York , 1980.
31 N. Gul, S. Kumar, B. Ahmad, R. H. Khan and Kabir-ud-Din, *Colloids Surf. B*, 2006, **51**, 10.
32 Z. Yaseen, S. U. Rehman, M. Tabish and Kabir-ud-Din, *J. Mol. Liquids*, 2014, **97**, 322.
33 L. Sreejith,, S. Parathakkat, S. M. Nair, S. Kumar, G. Varma, P. A. Hassan and Y. Talmon, *J. Phys. Chem.* B,2011, **115**, 464.
34 H. Yin, Z. Zhou, J. Huang, R. Zheng and Y. Zhang, *Angew. Chem. Int. Ed.*, 2003, **42**, 2188.
35 T. S. Davies, A. M. Ketner and S.R.Raghavan, *J. Am. Chem. Soc.*, 2006, **128**, 6669.
36 B. Jeong, K. M. Lee, A. Gutowska and Y. H. H. An, *Biomacromolcules*, 2002, **3**, 865.
37 C. W. Kan, E. A. S. Doherty and A.E. Barron, *Electrophoresis*, 2003, **24**, 4161.
38 T. N. C. Dantas, V. C. Santanna, A. A. D. Neto, E. L. B. Neto and M. Moura, *Colloid Surf. A.*,2003, **225**, 129.
39 P. Mukerjee, Edited by K. L. Mittal Solution Chemistry of Surfactants, Plenum, New York, 1979, p153.
40 P. M. Lindemuth and G. L. Bertrand, *J. Phys. Chem.*,1993, **97**, 7769.
41 Kabir-ud-Din, D. Bansal and S. Kumar, *Langmuir*, 1997, **13**, 5071.
42 H. H. Kohler and J. Stranad, *J. Phys. Chem.*, 1990, **94**, 7628.
43 A. Desai , D. Varade , J. Mata, V. Aswal and P. Bahadur, *Colloids and Surfaces* A, 2005, **259**, 111.
44 T. S. Davies, A. M. Ketner and S. R. Raghavan, *J. Am. Chem. Soc.*, 2006, **128**, 6669.
45 B. A. Schubert, E. W. Kaler and N. J. Wagner, *Langmuir*, 2003, **19**, 4079.
46 R. Zana and E. Waler, Giant Micelles: Properties and Applications, CRC Press, 2007.
47 J-H. Lee, J. P. Gustin, T. Chen, G. F. Payne and S. R. Raghavan, *Langmuir*, 2005, **21**, 26.
48 Y. I. Gonzalez, H. Nakanishi, M. Stjerndahl and E. W. Kaler, *J. Phys. Chem.* B, 2005, **109**, 11675.
49 N. Akter, S. Radiman, F. Mohamed, I. A. Rahman and M. I. H. Reza, *Sci Rep*., 2011,**1**,71.
50 S. R. Raghavan and E. W. Kaler, *Langmuir*, 2001, **17**, 300.
51 S. R. Raghavan, G. Fritz and E. W. Kaler, *Langmuir*, 2002, **18**, 3797.
52 M. E. Cates and S. J. Candau, *J. Phys. Condens. Matter*, 1990, **2**, 6869.
53 F. Kern, F. Lequeux, R. Zana and S. J. Candau, *Langmuir*, 1994, **10**, 1714.
54 P. Koshy, V. K. Aswal, M. Venkatesh and P. A. Hassan, *J. Phys. Chem.* B, 2011, **115**, 10817.
55 H. Rehage and H. Hoffman, *Mol. Phys.*, 1991, **74**, 933.
56 R. Ganapathy and A. K. Sood, *Langmuir*, 2006, **22**, 11016.
57 Spenley, N. A.; Cates, M. E.; MacLeish, T. C. B. *Phys. Rev. Lett.*,1993, **71**, 939.
58 R. Abdel-Rahem , M. Gradzielski , H. Hoffmann, *J. Colloid and Interface Sci.*, 2005, **288**, 570.
59 M. Aratono, N. Onimaru, Y. Yoshikai, M. Shigehisa, I. Koga, K. Wongwailikhit, A. Ohta, T. Takiue, B. Lhoussaine, R. Strey, Y. Takata, M. Villeneuve and H. Matsubara, *J. Phys. Chem.* B, 2007, **111**, 107.
60 R. G. Shrestha,, L. K. Shrestha, T. Matsunaga, M. Shibayama and K. Aramaki, *Langmuir*, 2011, **27**, 2229.
61 G. C. Kalur, B. D. Frounfelker, B. H. Cipriano, A. I. Norman and S. R. Raghavan, *Langmuir*, 2005, **21**, 10998.